

The Distribution of Mass in the Orion Dwarf Galaxy

N. Frusciante^{1*}, P. Salucci^{1†}, D. Vernieri^{1‡}, J. M. Cannon^{2§}, E. C. Elson^{3¶}

¹SISSA/ISAS, International School for Advanced Studies, Via Bonomea 265, 34136, Trieste, Italy;

INFN, Sezione di Trieste, Via Valerio 2, 34127, Trieste, Italy

²Department of Physics & Astronomy, Macalester College, 1600 Grand Avenue, Saint Paul, MN 55105, USA

³International Centre for Radio Astronomy Research, The University of Western Australia, M468, 35 Stirling Highway, Crawley, WA 6009, Australia

7 November 2021

ABSTRACT

Dwarf galaxies are good candidates to investigate the nature of Dark Matter, because their kinematics are dominated by this component down to small galactocentric radii. We present here the results of detailed kinematic analysis and mass modelling of the Orion dwarf galaxy, for which we derive a high quality and high resolution rotation curve that contains negligible non-circular motions and we correct it for the asymmetric drift. Moreover, we leverage the proximity ($D = 5.4$ kpc) and convenient inclination (47°) to produce reliable mass models of this system. We find that the Universal Rotation Curve mass model (Freeman disk + Burkert halo + gas disk) fits the observational data accurately. In contrast, the NFW halo + Freeman disk + gas disk mass model is unable to reproduce the observed Rotation Curve, a common outcome in dwarf galaxies. Finally, we attempt to fit the data with a MODified Newtonian Dynamics (MOND) prescription. With the present data and with the present assumptions on distance, stellar mass, constant inclination and reliability of the gaseous mass, the MOND “amplification” of the baryonic component appears to be too small to mimic the required “dark component”. The Orion dwarf reveals a cored DM density distribution and a possible tension between observations and the canonical MOND formalism.

Key words: Dark Matter; Galaxy: Orion dwarf; Mass profiles

1 INTRODUCTION

The measurement of the Rotation Curves (RCs) of disk galaxies is a powerful tool to investigate the nature of Dark Matter (DM), including its content relative to the baryonic components and their distributions. In particular, dwarf galaxies are good candidates to reach this aim as their kinematics are generally dominated by the dark component, down to small galactocentric radii (Persic et al. 1996; Gentile et al. 2004; de Blok et al. 2001; Oh et al. 2008; Salucci et al. 2008). This leads to a reliable measurement of the dynamical contribution of the DM to the RC and hence of its density profile. Therefore, a dwarf galaxy like the Orion dwarf provides us with an important test as to whether DM density profiles arising in Λ Cold Dark Matter (Λ CDM) numerical simulations (Navarro et al. 1996) are compatible with those detected in actual DM halos around galaxies. Let us comment that NFW profile arises from pure N-body DM simu-

lations. It is well known that, as effect of the baryonic infall in the cosmological DM halos and of the subsequent process of stellar disk formation, shallower profiles of the DM halo may arise (see Governato et al. (2010, 2012); Maccio’ et al. (2012)).

Recent studies of the RCs of dwarf galaxies have tested the NFW scenario. It is now clear that kinematic data are better fitted by a DM halo with a constant density core (e.g. Borriello & Salucci (2001); van den Bosch & Swaters (2001); de Blok et al. (2001); Woldrake et al. (2003); Gentile et al. (2004); Simon et al. (2005); Oh et al. (2008)), than by one that is centrally peaked. One specific example is DDO 47, whose velocity field is clearly best fitted if the DM halo is cored; moreover, its (small) detected non-circular motions cannot account for the discrepancy between data and the NFW predictions (Gentile et al. 2005).

The present investigation examines the DM content of the Orion dwarf galaxy. This nearby system harbors an extended H I disk, and thus provides us with an important test of the above paradigm. As we show below, the Orion dwarf is one of the few known galaxies whose kinematics *unambiguously* point towards a cored profile. This system is thus critically important for investigating the nature of the DM particle

* E-mail: noemi.frusciante@sissa.it

† E-mail: paolo.salucci@sissa.it

‡ E-mail: daniele.vernieri@sissa.it

§ E-mail: jcannon@macalester.edu

¶ E-mail: ed.elson@uwa.edu.au

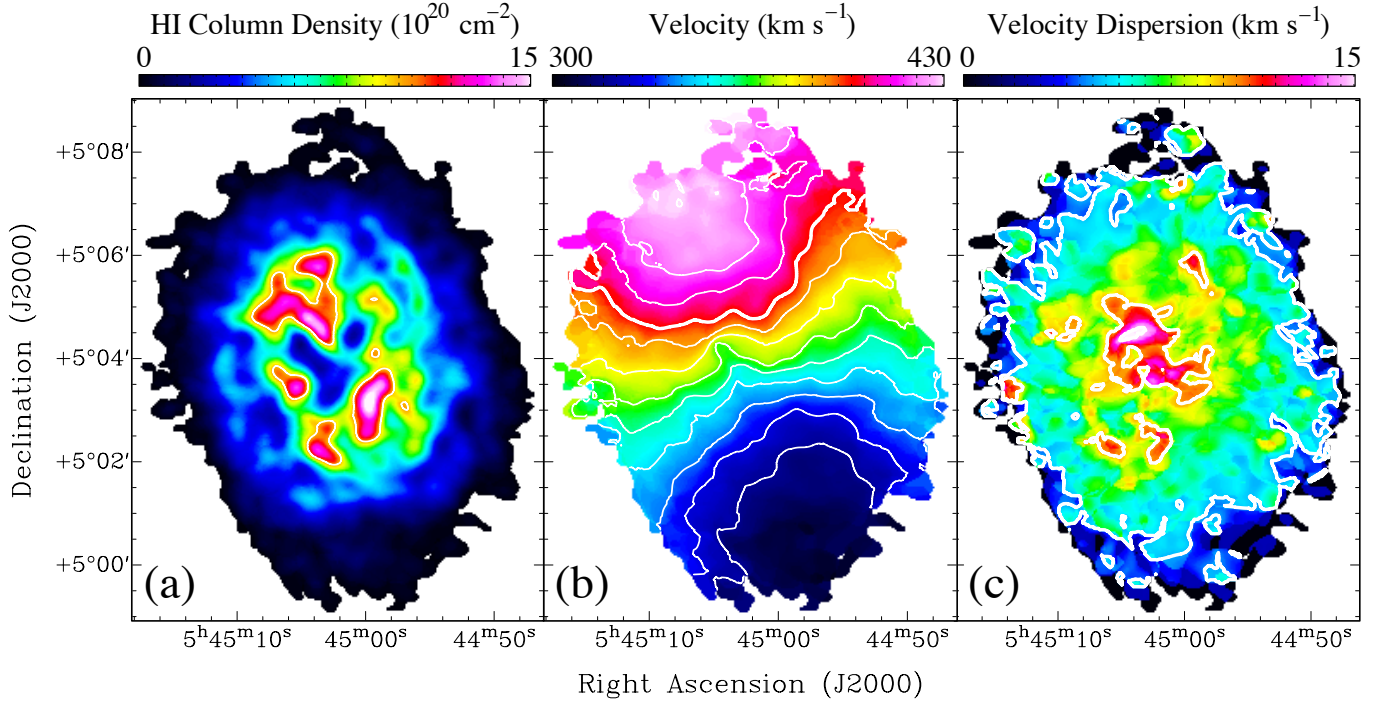


Figure 1. Comparison of the H I column density distribution (a), the intensity-weighted velocity field (b), and the intensity-weighted velocity dispersion (c); the beam size is $20''$. The contour in (a) is at the 10^{21} cm^{-2} level; the contours in (b) show velocities between 320 and 420 km s^{-1} , separated by 10 km s^{-1} , and the thick white line corresponds to the 400 km s^{-1} contour; the contours in (c) are at the 5, 10, 15 km s^{-1} levels.

and of the evolution of DM halos.

MOND accounts for the evidence that RCs of spiral galaxies are inconsistent with the corresponding distribution of the luminous matter (Milgrom 1983a,b). Rather than postulating the existence of a dark halo made by massive collisionless elementary particles, this scenario advocates that the gravitational force at low accelerations leaves the standard Newtonian regime to enter a very different one. Historically MOND has generally been successful in reproducing the RCs of spiral galaxies with only the (observed) luminous matter (e.g. Sanders (1996); Sanders & Verheijen (1998); Sanders & Noordermeer (2007)). However, cases of tension between data and the MOND formalism do exist (Gentile et al. 2004). It is important to stress that in order to derive the DM density profile or to test the MOND formalism, we must know the distribution of the ordinary baryonic components, as well as have reliable measurements of the gas kinematics. For the Orion dwarf, 21-cm H I surface brightness and kinematics have recently been published (Cannon et al. 2010): their analysis provides a high quality, high resolution RC, that, in addition, can be easily corrected for asymmetric drift and tested for non-circular motions. This galaxy is a very useful laboratory in that a simple inspection of the RC ensures us that it shows a large mass discrepancy at all radii. Moreover, the baryonic components are efficiently modeled (i.e., no stellar bulge is evident and the stellar disk shows a well-behaved exponential profile, see Vaduvescu et al. (2005)). The distance to the galaxy, which is critical for an unambiguous test of MOND (Sanders & McGaugh 2002), is estimated to be $5.4 \pm 1.0 \text{ Mpc}$ (Vaduvescu et al. 2005). It is important to stress that the distance of the Orion dwarf remains a significant source of uncertainty. Vaduvescu et

al. (2005) estimate the distance using the brightest stars method. The intrinsic uncertainty in this technique may allow a distance ambiguity much larger than the formal errors estimated by Vaduvescu et al. (2005), because in their work this method yields a scatter as large as 50% in distance. Finally, the system’s inclination (47°) is kinematically measured (see Section (3.1)) and is high enough to not affect the estimate of the circular velocity. The properties described above make the Orion dwarf galaxy an attractive candidate to determine the underlying gravitational potential of the galaxy.

This paper is organized as follows. In Sec. 2 we present the stellar surface photometry. In Sec. 3, the H I surface density and kinematics data are presented and discussed; we also provide the analysis of possible non-circular motions of the neutral gas. In Sec. 4 we model the RC in the stellar disk using a cored/cusped halo framework. In Sec. 5 we test the Orion kinematics against the MOND formalism. Our conclusions are given in Sec. 6.

2 STELLAR PHOTOMETRY

Following the discussion in Cannon et al. (2010), the underlying stellar mass in the Orion dwarf is estimated using the near-infrared (IR) photometry (J and K_S bands) presented by Vaduvescu et al. (2005). Those authors find $(J - K_S) = +0.80$ and a total K_S magnitude of $+10.90$. When comparing to models (see below) we assume that the color difference between K and K_S is negligible; further, we assume $L_{K, \odot} = +3.33$ (Cox 2000; Bessel 1979). Accounting for extinction, the total K-band luminosity of the Orion dwarf

is $\sim 3.5 \times 10^8 L_{\odot}$. The mass of the stellar component was estimated by Cannon et al. (2010) to be $(3.7 \pm 1.5) \times 10^8 M_{\odot}$. The stellar surface brightness profile is well fitted by an exponential thin disk, with a scale length of $R_D = 25'' \pm 1''$ (equivalent to 1.33 ± 0.05 kpc at the adopted distance). Moreover, there are no departures from an exponential profile that would be indicative of a prominent central bulge.

3 HI SURFACE DENSITY AND KINEMATICS

H I spectral line imaging was acquired with the *Very Large Array* and presented in Cannon et al. (2010). We refer the reader to that work for a full discussion of the data handling, and we summarize salient details here. The final data cubes have a circular beam size of $20''$, with a 3σ H I column density sensitivity of $N_{\text{HI}} = 1.5 \times 10^{19} \text{ cm}^{-2}$. The first three moment maps (i.e. the integrated H I intensity, the velocity field, and the velocity dispersion) are shown in Figure (1). The neutral gas disk of the Orion dwarf shows rich morphological and kinematic structure at this physical resolution. The outer disk contains tenuous H I gas, but column densities rise above the $5 \times 10^{20} \text{ cm}^{-2}$ level at intermediate radii. There is plentiful high-column density ($>10^{21} \text{ cm}^{-2}$) H I throughout the disk. The more or less parallel iso-velocity contours at inner radii are indicative of linear rotation (although almost certainly not solid body) and the curving of the outer contours suggests that the outer rotation curve has a fairly constant velocity. The outer disk contours show no evidence for a decrease in rotational velocity at large radii. In the central regions of the disk, however, some H I “holes” or “depressions” manifest a pronounced kink in these contours (consider the contours at $370 \pm 20 \text{ km s}^{-1}$). The intensity weighted velocity dispersion averages to $\sim 7\text{--}8 \text{ km s}^{-1}$ throughout the disk, although the innermost regions show dispersions above 10 km s^{-1} .

The total H I flux integral, proportional to the H I disk mass, was found to be $50.3 \pm 5.1 \text{ Jy km s}^{-1}$, a value somewhat lower than the single-dish flux measure of $80.6 \pm 7.72 \text{ Jy km s}^{-1}$ by Springob et al. (2005); the difference may arise from the lack of short interferometric spacings that provide sensitivity to diffuse structure. The total H I mass is found to be $M_{\text{HI}} = (3.5 \pm 0.5) \times 10^8 M_{\odot}$. After applying the usual 35% correction for Helium and molecular material, we adopt $M_{\text{gas}} = (4.7 \pm 0.7) \times 10^8 M_{\odot}$ as the total gas mass.

In Figure (2) we plot the $10''/20''$ resolution H I surface density, throughout the gas disk. A simple fit (valid out to the last measured point and for the scope of this work) yields:

$$\mu_{\text{HI}}(r) = \frac{-0.263r^3 + 1.195r^2 + 3.094r + 18.549}{0.154r^3 - 1.437r + 6.703} M_{\odot}/pc^2, \quad (1)$$

where r is in kpc. The related fitting uncertainty on $\mu_{\text{HI}}(r)$ is about 20%. Figure (2) shows that the H I surface density rises from the center of the galaxy, reaches a maximum, and then declines exponentially. At the last measured point, i.e. out to ~ 7 kpc, the profile has almost (though not completely) reached the edge of the H I disk and rapidly converges to zero. Note that, in Newtonian gravity, the outer gaseous disk contributes in a negligible way to the galaxy total gravitational potential.

3.1 The Circular Velocity

The channel maps of the Orion dwarf provide evidence of well-ordered rotation throughout the H I disk (see Cannon et al. 2010). The intensity-weighted-mean velocity field (Figure (1b)) exhibits symmetric structure in the outer disk. Twisted iso-velocity contours at inner radii coincide with the H I holes near the centre of the disk. The disk is therefore dominated by circular motion. The RC of the galaxy was derived by fitting a tilted ring model to the intensity-weighted-mean velocity field using the GIPSY task ROTCUR. The routine carries out a least-squares fit to V_{los} , the line of sight-velocity. To derive the best-fitting model, an iterative approach was adopted in which the various combinations of the parameters were fitted. The final RC was extracted by fixing all other parameters. The receding and approaching sides of the galaxy were fitted separately. The best fitting parameters are $i = (47 \pm 3)^{\circ}$, $P.A. = (20 \pm 2)^{\circ}$, $V_{\text{sys}} = 368.5 \pm 1.0 \text{ km/s}$, and $(\alpha_{2000}, \delta_{2000}) = (05:45:01.66, 05:03:55.2)$ for the dynamical centre. We have realized that the inclination is not dependent on the radius, and the fit is shown in Figure (3). Its weighted value is $(46.8 \pm 0.14)^{\circ}$. Notice that because the errors reported by GIPSY/ROTCUR include only errors on the fits and systematics are not included, the 3° error estimate comes from attempting the ROTCUR fits in various orders (e.g., holding each variable fixed in turn).

The resulting RC is shown in Figure (4). Notice that in this object the disk inclination is determined kinematically and therefore it is quite accurate. No result of this paper changes by adopting different values of i , inside the quoted errorbar.

The second-order moment map for the galaxy is shown in Figure (1c). Throughout most of the disk, the velocity dispersion is roughly constant at $\sigma \simeq 7 \pm 2 \text{ km/s}$, with a more complex behaviour near the galaxy centre and at the outermost radii. This velocity dispersion estimate allows us to derive the asymmetric drift correction to the RC yielded by the tilted ring model. The observed rotation velocity, V_{rot} , is related to the circular velocity V_c via

$$V_c^2(r) = V_{\text{rot}}^2(r) - \sigma^2(r) \left[\frac{d \log \mu_{\text{HI}}(r)}{d \log r} + \frac{d \log \sigma^2(r)}{d \log r} \right]. \quad (2)$$

From an examination of Figure (4) it is clear that the V_{rot} and V_c profiles differ by less than 1%. Throughout this paper, we use the latter for the purposes of mass modelling. We notice that in very small dwarfs this correction is not negligible ($V_{\text{rot}} \sim \sigma$) and it introduces an uncertainty in the analysis, e.g. Begum & Chengalur (2004).

In summary, the Orion dwarf RC has a spatial resolution of 0.26 kpc (i.e. $0.2 R_D$), and extends out to $5.1 R_D$. The uncertainties on the RC are few km/s and the error on the RC slope $d \log V / d \log R < 0.1$.

Is the circular velocity given by eq. (2) a proper estimate of the gravitational field? To further investigate the presence of non-circular motions within the H I disk that jeopardize the kinematics, we carried out a harmonic decomposition of the intensity-weighted velocity field to search for any significant non-circular components. This test is necessary in that the undetected presence of non-circular motions can lead to incorrect parametrization of the total mass distribution. Following Schoenmakers et al. (1997), the line-of-sight velocities from the H I velocity field are decomposed into har-

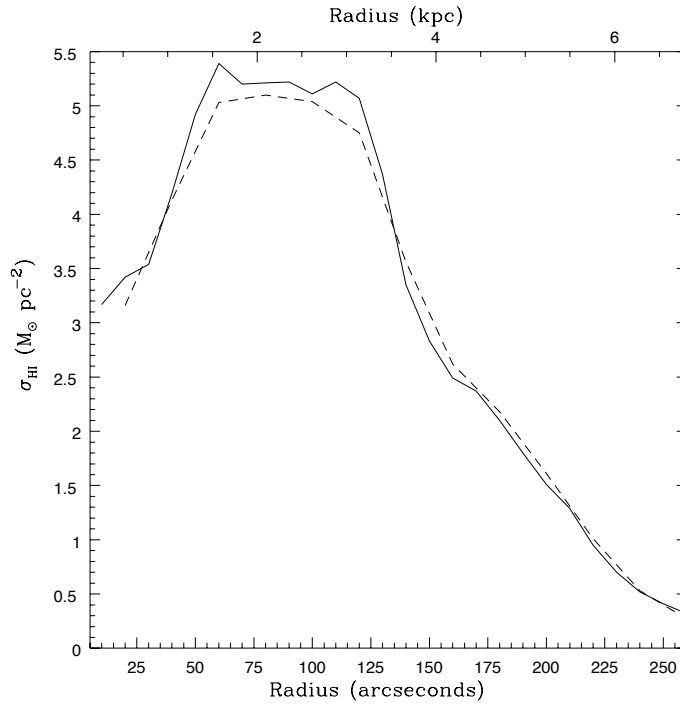


Figure 2. Radially averaged H I mass surface density profiles of the Orion dwarf, created by averaging H I emission in concentric rings emanating from the dynamical center found in our RC analysis. The solid/dotted lines were created from the 10'' /20'' resolution images.

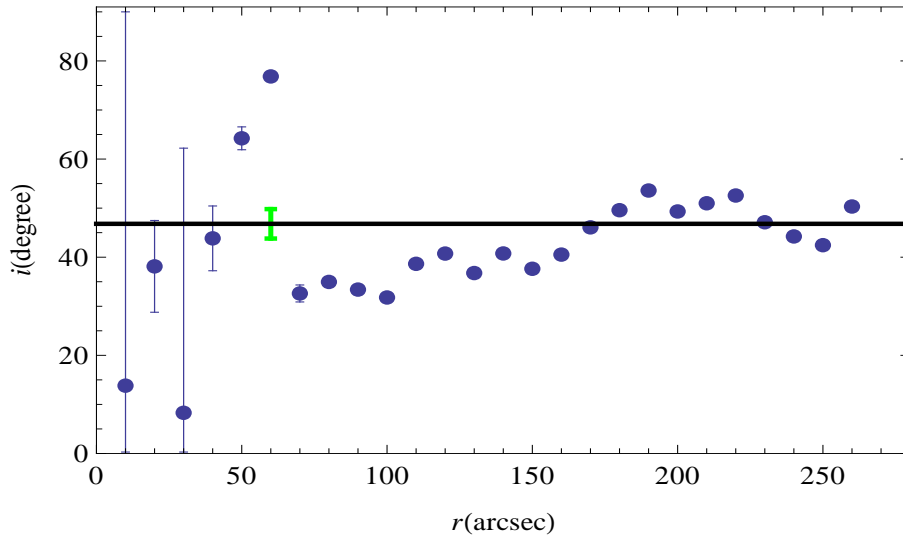


Figure 3. Inclination best fit (thick Black line) for high resolution (10'') data (filled Blue points). Errorbars are plotted and in most cases are smaller than the symbol size. The errors reported (by GIPSY/ROTCUR) include only errors on the fits, while the systematic error considered (3°) is shown as a Green errorbar.

monic components up to order $N = 3$ according to

$$V_{los} = V_{sys} + \sum_{m=1}^3 c_m \cos m\theta + s_m \sin m\theta, \quad (3)$$

where V_{sys} is the systemic velocity, c_m and s_m are the magnitudes of the harmonic components, m the harmonic number, and θ the azimuthal angle in the plane of the galaxy. The GIPSY task RESWRI was used to carry out the decomposition by fitting a purely circular model to the velocity field, subtracting it from the data, and then determining

from the residual the magnitudes of the non-circular components. The tilted ring model fitted by RESWRI had its kinematic centre fixed to that of the purely circular tilted ring model used to derive the RC above. The position angles and inclinations were fixed to constant values of 20 and 47°, respectively.

The parameters of the best-fitting model are shown in Figure (5). Adjacent points are separated by a beam width in order to ensure that they are largely independent of one another. We argue that because the standard tilted ring

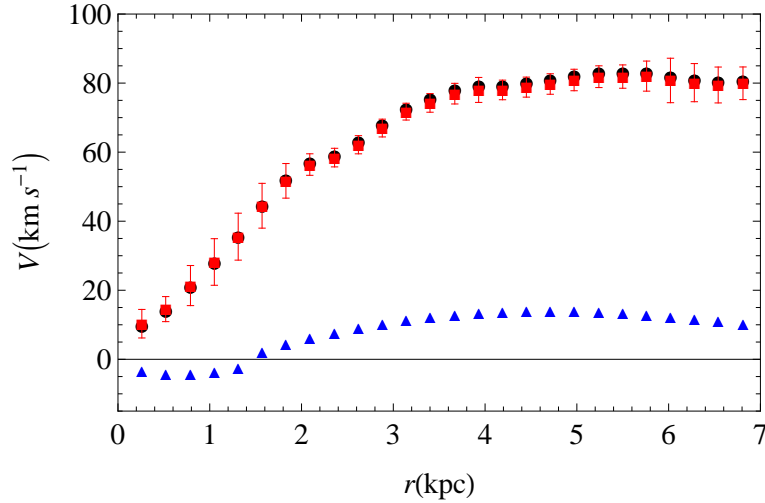


Figure 4. Rotation velocity corrected for asymmetric drift (filled black points), raw velocity data with error bars (filled red boxes) and the asymmetric drift correction (filled blue triangles).

model has fewer free parameters than the model incorporating the higher order Fourier components, it is not as essential to space the points on the rotation curve by a full beam width. Then in this model only 16 points are considered instead of the 26 points used in fitting the RC.

At inner radii the inferred non-circular motions are not negligible, but this is almost certainly due to the fact that the H I distribution over this portion of the disk is irregular, being dominated by the large central H I under-densities. The harmonic components of the outer disk are, instead, reliable and demonstrate the gas flow to be dominated by circular kinematics. The circular velocity so obtained well matches that found by means of the tilted ring model presented above. The amplitudes of c_2 and s_2 are too small to hide a cusp inside an apparently solid body RC (as suggested by Hayashi & Navarro (2006)). These results provide further decisive support for the use of V_{rot} of the Orion dwarf as a tracer of its mass distribution.

4 MASS MODELING

We model the Orion dwarf as consisting of two “luminous” components, namely the stellar and the gaseous disks, embedded in a dark halo. The stellar component is modelled as an exponential thin disk (Freeman 1970) with a scale length of 1.33 kpc. Any bulge component is assumed to be negligible in terms of mass. The dynamical contribution of the gas to the observed RC is derived from the H I total intensity map. A scaling factor of 1.33 is incorporated to account for the presence of Helium and other elements. For the dark halo we consider two different parametrizations of the mass distribution: an NFW profile (Navarro et al. 1996) and the cored profile of the Halo Universal Rotation Curve (URCH) (Salucci et al. 2007). It is well known that the NFW profile is one outcome in numerical simulations of cold dark matter structure formation, whereas the cored profile (an empirical result), by design, fits the broad range of RC shapes of spiral galaxies.

4.1 Mass Models: stellar disk + dark matter halo

The RC is modelled as the quadrature sum of the RCs of the individual mass components:

$$V_{mod}^2 = V_D^2 + V_{DM}^2 + V_{gas}^2. \quad (4)$$

For the cored halo parametrization we adopt the URCH profile:

$$V_{URCH}^2(r) = 6.4 \frac{\rho_0 r_0^3}{r} \left[\ln \left(1 + \frac{r}{r_0} \right) - \arctan \left(\frac{r}{r_0} \right) \right] + \frac{1}{2} \ln \left(1 + \frac{r^2}{r_0^2} \right), \quad (5)$$

where the disk mass, the core radius r_0 and the central halo density ρ_0 are free parameters.

It is evident that this model yields a total RC that fits the data extremely well (see Figure (6) left panel), with best-fitting parameters of $r_0 = (3.14 \pm 0.32)$ kpc, $M_D = (3.5 \pm 1.8) \times 10^8 M_\odot$ and $\rho_0 = (4.1 \pm 0.5) \times 10^{-24} \text{g/cm}^3$. More accurate statistics is not necessary; the mass model predicts all the $V(r)$ data points within their observational uncertainty.

Notice that the derived value of the disk mass agrees with the photometric estimate discussed above. The corresponding virial mass and radius of the DM halo are $M_{vir} = (5.2 \pm 0.5) \times 10^{10} M_\odot$ (see eq. 10 in Salucci et al. (2007)) and $R_{vir} = 95.5_{-4}^{+5}$ kpc (Eke et al. 1996), respectively. We note that the Orion dwarf has a mass 20 times smaller than that of the Milky Way, with the DM halo dominating the gravitational potential at all galactocentric radii. The baryonic fraction is $f_b = (M_D + M_{gas})/M_{vir} = 0.016$, while the gas fraction is $M_{gas}/M_{vir} = 9 \times 10^{-3}$.

The RC for the NFW dark matter profile is

$$V_{NFW}^2(r) = V_{vir}^2 \frac{g(c)}{xg(cx)}, \quad (6)$$

where $x = r/R_{vir}$, $g(c) = [\ln(1+c) - c/(1+c)]^{-1}$ and $c(M_{vir}) = 9.60 (M_{vir}/10^{12} h^{-1} M_\odot)^{-0.075}$ is the concentration parameter (see Klypin et al. (2011)). We fitted the RC

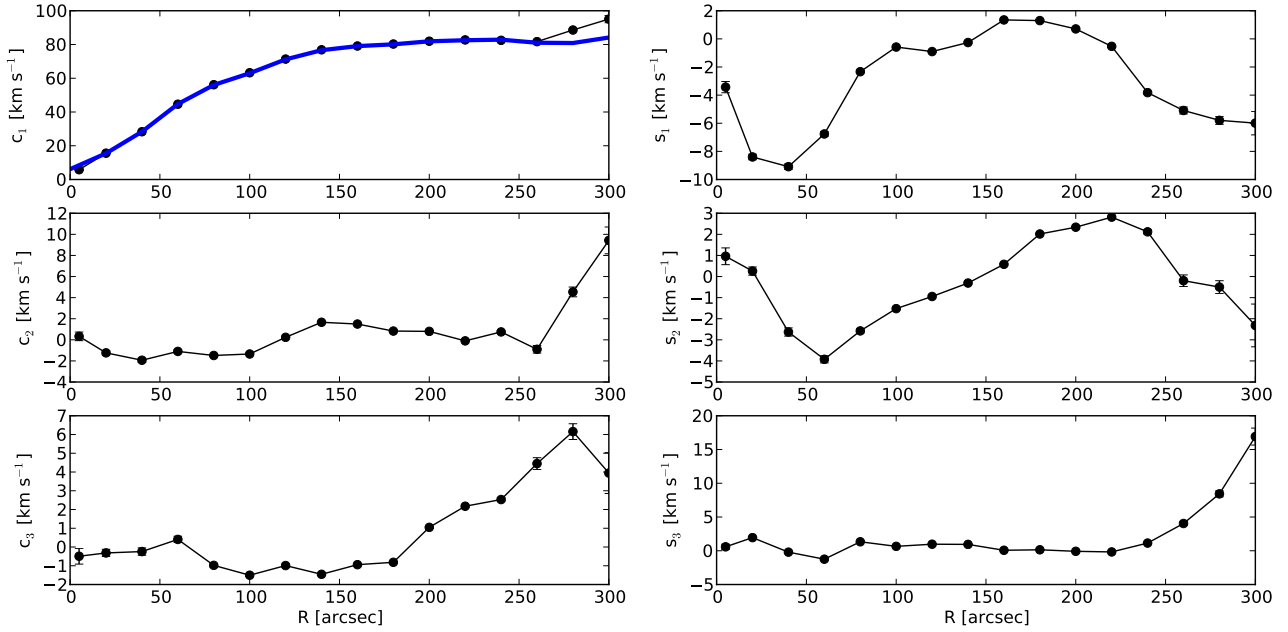


Figure 5. Non-circular velocity components as derived by carrying out a harmonic decomposition of the intensity-weighted-mean velocity field. The c_1 profile corresponds to the circular RC. The RC derived by fitting tilted ring model to the intensity-weighted-mean velocity field is shown as a solid blue curve.

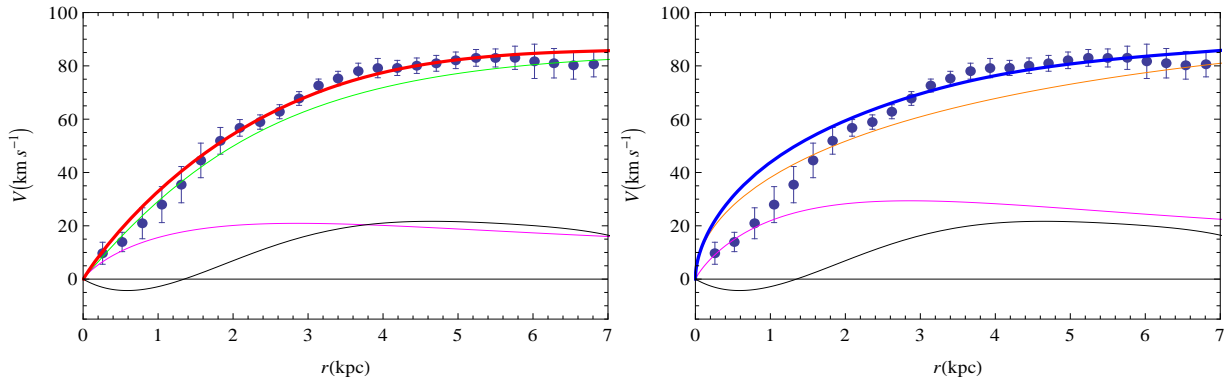


Figure 6. Left: URC model of Orion dwarf. The circular velocity (filled circles with error bars) is modeled (thick Red line) by a Freeman disk (Magenta line), a URCH halo (Green line), and the H I circular velocity (Black line). Right: NFW model of Orion dwarf. The circular velocity data (filled circles with error bars) is modeled (thick Blue line) including a Freeman disk profile (Magenta line), a NFW halo profile (Orange line) and the H I circular velocity (Black line). In both cases the values of the free parameters are reported in the text.

of the Orion dwarf by adjusting M_{vir} and M_D . The resulting best-fit values are $M_{vir} = (2.5 \pm 0.5) \times 10^{11} M_{\odot}$ and $M_D = (6.9 \pm 1.7) \times 10^8 M_{\odot}$, but since $\chi^2_{red} \simeq 3.3$, i.e. the fit is unsuccessful, the best-fit values of the free parameters and those of their fitting uncertainties do not have a clear physical meaning. We plot the results in the right panel of Figure (6). The NFW model, at galactocentric radii $r < 2$ kpc, overestimates the observed circular velocity (see Figure (6) right panel).

5 ORION KINEMATICS IN THE MOND CONTEXT

An alternative to Newtonian gravity was proposed by Milgrom (1983a) to explain the phenomenon of mass discrepancy in galaxies. It was suggested that the true acceleration a of a test particle, at low accelerations, is different from the standard Newtonian acceleration, a_N :

$$a = \frac{a_N}{\mu(a/a_0)}, \quad (7)$$

where $\mu(a/a_0)$ is an interpolation function and $a_0 = 1.35 \times 10^{-8} \text{cm s}^{-2}$ is the critical acceleration at which the transition occurs (see Famaey et al. (2007)). For this we adopt the following form of the interpolation function (see Famaey &

Binney (2005)):

$$\mu(a/a_0) = \frac{a/a_0}{1 + a/a_0}. \quad (8)$$

In this framework the circular velocity profile can be expressed as a function of a_0 and of the standard Newtonian contribution of the baryons to the RC, $V_{bar} = (V_D^2 + V_{gas}^2)^{1/2}$, obtaining for it

$$V_{MOND}^2 = V_{bar}^2(r) \left(\frac{\sqrt{1 + \frac{4a_0 r}{V_{bar}^2(r)} + 1}}{2} \right), \quad (9)$$

(see Richtler et al. (2008)). Eq. (9) shows that in the MOND framework the resulting RC is similar to the no-DM standard Newtonian one, with an additional term that works to mimic and substitute for the DM component (Sanders & McGaugh 2002). No result of this paper changes by adopting the “standard” MOND interpolation function (see Zhao & Famaey (2006)).

The best-fitting MOND mass model is shown in Figure (7). The model total RC (cyan line) completely fails to match the observations. We fix the stellar mass M_D at $M_D = 2.6 \times 10^8 M_\odot$. If we let the disk mass becomes higher, covering the mass range estimated in Cannon et al. (2010), the fit is not even able to reproduce the RC at inner radii. Note that in the MOND formalism, the distance of the galaxy and the amount of gaseous mass are both crucial in deriving the model RC. To quantify the discrepancy of these observations with the MOND formalism, note that only if the Orion dwarf were 1.9 times more distant than the current estimate we would obtain a satisfactory fit to the RC (see Figure (8)).

6 CONCLUSIONS

The Orion dwarf galaxy is representative of a population of dwarfs with a steep inner RC that gently flattens at the edge of the gas disk. The observed kinematics imply the presence of large amounts of DM also in the central regions. We have used new H I observations of the Orion dwarf to analyze its kinematics and derive the mass model. The derived RC is very steep and it is dominated by DM at nearly all galactocentric radii. Baryons are unable to account for the observed kinematics and are only a minor mass component at all galactic radii.

We have used various mass modeling approaches in this work. Using the NFW halo, we find that this model fails to match the observed kinematics (as occurs in other similar dwarfs). We show that non-circular motions cannot resolve this discrepancy. Then we modelled the galaxy by assuming the URCH parametrization of the DM halo. We found that this cored distribution fits very well the observed kinematics. Orion is a typical dwarf showing a cored profile of the DM density and the well-known inability of DM halo cuspy profiles to reproduce the observed kinematics. Finally, we find that the MOND model is discrepant with the data if we adopt the literature galaxy distance and gas mass. The kinematic data can be reproduced in the MOND formalism if we allow for significant adjustments of the distance and/or value of the gas mass. Let us point out that the present interferometric observations may miss some of the objects’ H I

flux, although this may be limited in that the cubes do not have significant negative bowls. Obviously, for bigger values of the H I mass, the distance at which the baryon components would well fit the data will also somewhat decrease. It is worth stressing that there is a galaxy distance (albeit presently not-favoured) for which MOND would strike an extraordinary success in reproducing the observed kinematics of the Orion dwarf.

The Orion dwarf has a favorable inclination, very regular gas kinematics, a small asymmetric drift correction, a well-understood baryonic matter distribution, and a large discrepancy between luminous and dynamical mass. All of these characteristics make this system a decisive benchmark for the MOND formalism and a promising target for further detailed studies. Of particular value would be a direct measurement of the distance (for example, infrared observations with the Hubble Space Telescope would allow a direct distance measurement via the magnitude of the tip of the red giant branch).

ACKNOWLEDGMENTS

The authors would like to thank the referee, Gianfranco Gentile, for his very fruitful comments that have increased the level of presentation of the paper.

REFERENCES

- Begum A. & Chengalur J. N., 2004, *A&A*, 413, 525
 Bessell M. S., 1979, *PASP*, 91, 589
 Borriello A. & Salucci P., 2001, *MNRAS*, 323, 2, 285
 Cannon J. M., Haynes K., Most H., Salzer J. J., Haugland K., Scudder J., Sugden A., Weindling J., 2010, *AJ*, 139, 2170
 Cox A. N., 2000, *Allens Astrophysical Quantities* (4th ed.; New York; Springer)
 de Blok E., McGaugh S., Rubin V. C., 2001, *ApJ*, 122, 2396
 Eke V. R., Cole S., Frenk C. S., 1996, *MNRAS*, 282, 263
 Famaey B. & Binney J., 2005, *MNRAS*, 363, 603
 Famaey B., Gentile G., Bruneton, J. P., Zhao H. S., 2007, *Phys. Rev. D*, 75, 063002
 Freeman K. C., 1970, *ApJ*, 160, 811
 Gentile G., Salucci P., Klein U., Vergani D., Kalberla P., 2004, *MNRAS*, 351, 903
 Gentile G., Burkert A., Salucci P., Klein U., Walter F., 2005, *ApJ*, 634, 2, L145
 Governato F., Brook C., Mayer L., Brooks A., Rhee G., Wadsley J., Jonsson P., Willman B., Stinson G., Quinn T., Madau P., 2010, *Nature*, 463, 203
 Governato F., Zolotov A., Pontzen A., Christensen C., Oh S. H., Brooks A. M., Quinn T., Shen S., Wadsley J., 2012, *arXiv:1202.0554v2* [astro-ph.CO]
 Hayashi E. & Navarro J. F., 2006, *MNRAS*, 373, 1117
 Klypin A. A., Trujillo-Gomez S., Primack J., 2011, *ApJ*, 740, 102
 Maccio’ A.V., Stinson G., Brook C.B., Wadsley J., Couchman H. M. P., Shen S., Gibson B. K., Quinn T., 2012, *ApJ*, 744, L9.
 Milgrom M., 1983a, *ApJ*, 270, 365
 Milgrom M., 1983b, *ApJ*, 270, 371

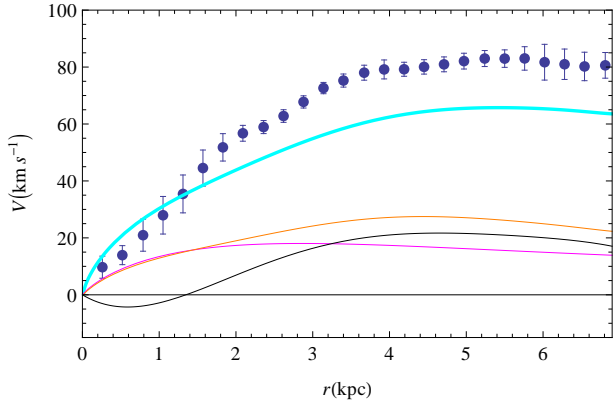


Figure 7. MOND model of Orion dwarf spiral. The circular velocity data (filled circles with error bars) is modeled with the MOND profile (thick Cyan line). Also shown are the (newtonian) Freeman disk contribution (Magenta line), the H I contribution (Black line) and the total baryonic contribution (Orange line).

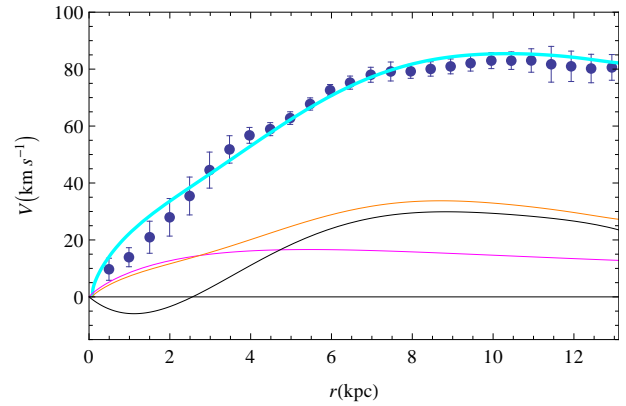


Figure 8. MOND model of Orion dwarf spiral for a distance from the galaxy of ~ 10 Mpc, a factor 1.9 farther than the nominal distance. The legend to the lines is the same of Figure 7. The resulting disk mass is $M_D = 4.2 \times 10^8 M_\odot$.

- Navarro J. F., Frenk C. S., White S. D. M., 1996, *ApJ*, 462, 563
 Oh S. H., de Blok W. J. G., Walter F., Brinks E., Kennicutt R. C. Jr., 2008, *AJ*, 136, 6, 2761
 Persic M., Salucci P., Stel F., 1996, *MNRAS*, 281, 271
 Richtler T., Schubert Y., Hilker M., Dirsch B., Bassino L., Romanowsky A. J., 2008, *A&A*, 478, L23
 Salucci P., Lapi A., Tonini C., Gentile G., Yegorova I., Klein U., 2007, *MNRAS*, 378, 41
 Salucci P., Yegorova I. A., Drory N., 2008, *MNRAS*, 388, 159
 Sanders R. H., 1996, *ApJ*, 473, 117
 Sanders R. H. & Verheijen M. A. W., 1998, *ApJ*, 503, 97
 Sanders R. H. & McGaugh S. S., 2002, *ARA&A*, 40, 263
 Sanders R. H. & Noordermeer E., 2007, *MNRAS*, 379, 702
 Schoenmakers R. H. M., Franx M., de Zeeuw P. T., 1997, *MNRAS*, 292, 349
 Simon Joshua D., Bolatto A. D., Leroy A., Blitz L., Gates E. L., 2005, *ApJ*, 621, 2, 757
 Springob C. M., Haynes M. P., Giovanelli R., Kent B. R., 2005, *ApJS*, 160, 1, 149
 Vaduvescu O., McCall M. L., Richer M. G., Fingerhut R. L., 2005, *AJ*, 130, 4, 1593
 van den Bosch F. C. & Swaters R. A., 2001, *MNRAS*, 325, 3, 1017
 Woldrake D. T. F., de Blok W. J. G., Walter F., 2003, *MNRAS*, 340, 1, 12
 Zhao H. S. & Famaey B., 2006, *ApJ*, 638, L9-L12